Environmental Science & Technology

Article

pubs.acs.org/est

# $SO_2$ Initiates the Efficient Conversion of $NO_2$ to HONO on MgO Surface

Qingxin Ma,*[,†,‡] Tao Wang,*[,†] Chang Liu,[§] Hong He,[‡] Zhe Wang,[†] Weihao Wang,[†] and Yutong Liang[†]

[†]Department of Civil and Environmental Engineering, The Hong Kong Polytechnic University, Kowloon, Hong Kong 999077, China

[‡]Research Center for Eco-Environmental Sciences, Chinese Academy of Sciences, Beijing 100085, China

[§]State Key Laboratory of Severe Weather & Key Laboratory of Atmospheric Chemistry of China Meteorological Administration, Chinese Academy of Meteorological Sciences, Beijing 100081, China

Supporting Information

**ABSTRACT:** Nitrous acid (HONO) is an important source of hydroxyl radical (OH) that determines the fate of many chemically active and climate relevant trace gases. However, the sources and the formation mechanisms of HONO remain poorly understood. In this study, the effect of $SO_2$ on the heterogeneous reactions of $NO_2$ on MgO as a mineral dust surrogate was investigated. The reactivity of MgO to $NO_2$ is weak, while coexisting $SO_2$ can increase the uptake coefficients of $NO_2$ on MgO by 2−3 orders of magnitude. The uptake coefficients of $NO_2$ on $SO_2$-aged MgO are independent of $NO_2$ concentrations in the range of 20−160 ppbv and relative humidity (0−70%RH). The reaction mechanism was demonstrated to be a redox reaction between $NO_2$ and surface sulfite. In the presence of $SO_2$, $NO_2$ was reduced to nitrite under dry conditions, which could be further converted to gas-phase HONO in humid conditions. These results suggest that the reductive effect of $SO_2$ on the heterogeneous conversion of $NO_2$ to HONO may have a significant contribution to the unknown sources of HONO observed in polluted areas (for example, in China).

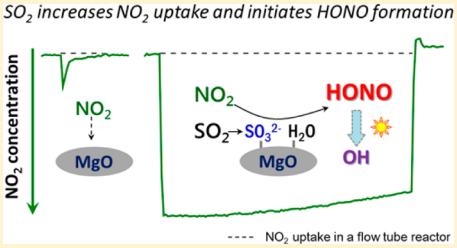


## INTRODUCTION

Nitrous acid (HONO) significantly enhances the atmospheric oxidative capacity due to the production of OH radical.[1] Field and modeling studies have shown that HONO photolysis contributes significantly to the OH production, with a total average contribution of up to 30−60% throughout the day.[2−4] Because OH radical is the primary oxidant in the atmosphere and a main scavenger of gaseous pollutants, HONO affects the fate of many chemically active and climate relevant gases as well as the formation of ozone and secondary aerosols. HONO is also an important indoor pollutant due to its negative health effects.[5,6] Therefore, investigation of HONO sources is of great environmental and health significance.

The currently known sources of HONO include direct emissions, gas-phase formation through the OH and NO reaction, heterogeneous reactions of $NO_2$ on the ground and particle surfaces, surface photolysis reactions, and biological processes.[1,3,7−15] Among these sources, it is well-accepted that heterogeneous processes involving conversion of $NO_2$ on wet surfaces are the major formation pathway of HONO in the atmosphere. For example, HONO was produced during the hydrolysis of $NO_2$ on surfaces such as mineral dust, glass, and buildings.[14,16−18] Redox reaction between $NO_2$ and soot was also proposed as a source of HONO.[19] Because the reactive sites on soot decreased quickly after exposure to $NO_2$, the contribution of this process to HONO sources greatly depends on the content of reactive compounds on surface.[20−23] A number of research projects have focused on the photo-enhanced conversion of $NO_2$ on surfaces such as soot,[11] humic acids,[24−26] organic compounds,[27,28] and $TiO_2$-containing mineral dust[29−32] due to their photocatalytic or photosensitive properties. These photochemical reactions of $NO_2$ on aerosol particles and ground surface have been considered as daytime HONO sources in the troposphere.[10,15]

Although the mechanism of $NO_2$ conversion to HONO on surfaces has been widely studied, the role of aerosol on the formation of HONO is still controversial. Observations of HONO in the United States and Europe concluded that the ground surface is the major source of HONO, and reactions on aerosol particles are considered less-important.[3,33−35] In contrast, the correlation between particulate matters and HONO were observed in the heavy haze episodes in China, and reactions on surfaces of high loading of aerosols were suggested as an important source of HONO.[36−39] However, the mechanism is yet to be corroborated by laboratory results.

Mineral dust is a major component of aerosol over the world[40,41] and particularly in China.[40,42,43] It is estimated that 1000−3000 Tg of mineral aerosols are emitted annually into the atmosphere.[44] Field measurements observed a large ratio of HONO to $NO_2$ during dust storms, suggesting the highly efficient conversion of $NO_2$ to HONO on mineral dust particles.[45] However, the true uptake coefficients of $NO_2$ on mineral dust are very low,[32,46,47] indicating that mineral dust is

Received: December 9, 2016
Revised: February 19, 2017
Accepted: February 27, 2017
Published: March 1, 2017





DOI: 10.1021/acs.est.6b05724
Environ. Sci. Technol. 2017, 51, 3767−3775

a minor medium for $NO_2$ reaction. Recently, a positive correlation (0.92) between gas-phase HONO and particulate sulfate was observed during dusty days,[48] and the authors attributed the correlation to a synergistic mechanism of adsorption and reaction between $NO_2$ and $SO_2$ on dust particles rather than the hydrolysis of $NO_2$. However, the mechanism is not clear yet. Oxidation of $SO_2$ or sulfite to sulfate in the presence of $NO_2$ in aqueous reactions has been considered as an important source of sulfate[49,50] in which $NO_2$ was converted to nitrite or $N_2O$ dependent on the reaction conditions.[50−54] Compared to the liquid phase, the interaction of $NO_2$ and $SO_2$ on the particle surface is more-complicated and not well-studied. For example, $NO_2$ was found to have little effect relative to air on the conversion of $SO_2$ to sulfate on carbon particles.[55] However, in Santis and Allegrini's study, the interaction of $SO_2$ and $NO_2$ with the carbonaceous materials led to sulfate and different nitrogen-containing species depending on the type of carbonaceous materials.[56] Previous studies indicated that heterogeneous reactions $SO_2$ and $NO_2$ on mineral particles exhibit synergistic effect and promote the formation of sulfate.[57−60] It should be noted that the concentrations of $SO_2$ or $NO_2$ used in these studies were much higher than atmospheric mixing ratios of these gases. Nevertheless, whether this synergistic effect relates to the formation of HONO is not clear. This inspired us to explore the effect of $SO_2$ on the conversion of $NO_2$ to HONO on mineral particles because minerals are ubiquitous in aerosol and soil.

$SO_2$ pollution is still severe in China due to the large combustion of fossil fuel. In haze episodes, the average concentration of $SO_2$ could be 60 ppbv, with the highest value close to 300 ppbv.[38] In the present study, we investigated the effect of coexisting $SO_2$ on the heterogeneous reaction of $NO_2$ on MgO using coated-wall flow tube reactor and in situ diffuse reflectance Fourier transformed infrared spectroscopy (in situ DRIFTS) at room temperature. MgO is an important component of mineral dust and soil, which has been always chosen as a representative of crustal oxides.[40,59,61−64] A possible mechanism of the effect of $SO_2$ on the uptake and transformation of $NO_2$ was proposed. This work will contribute to a better understanding of the sources of HONO in polluted regions as well as in dust storms.

## MATERIALS AND METHODS

**Samples.** MgO (Sigma-Aldrich) was used as purchased. A total mass of 1.0 g of MgO powder was dissolved in 20.0 mL of water. This suspension was dripped uniformly into a quartz tube (20.0 cm length, 1.1 cm i.d.) and dried overnight in an oven at 373 K. The resulting homogeneous film covered the entire inner area of the tube and was uniform in thickness. The specific surface area of the samples was measured to be 135.6 $cm^2\ mg^{-1}$ by nitrogen Brunauer−Emmett−Teller (BET) physisorption (Quantachrome Autosorb-1-C).

**Coated-Wall Flow Tube Reactor.** The uptake experiments were performed in a horizontal cylindrical coated-wall flow tube reactor (Figure S1), which has been described in detail elsewhere.[23,47] The flow tube reactor was covered with aluminum foil to avoid the influence of light in the room. The experiments were performed at ambient pressure and maintained at 295 K by circulating water bath through the outer jacket of the flow tube reactor. High-purity synthetic air was used as carrier gas, and the total flow rate introduced in the flow tube reactor was 0.9 $L{\cdot}min^{-1}$, ensuring a laminar regime. The relative humidity (RH) was recorded during the whole experiment by a hygrometer (Omega RH-USB). $NO_2$ with designing concentrations was introduced into the flow tube through a movable injector with 0.3 cm (o.d.) radius. The concentrations of $NO_2$ and NO were online measured using two chemiluminescence analyzers (THERMO 42i). One analyzer used a molybdenum oxide (MoO) catalyst that coverts $NO_2$, HONO, and other reactive nitrogen species, while the other is coupled with a highly selective photolytic converter that photodissociates $NO_2$ to NO at wavelengths of 380−410 nm (Droplet Measurement Technologies, model BLC).[65] The difference between these two analyzers is due to the existence of HONO, which was confirmed by comparative measurement of HONO with a long-path absorption photometer (LOPAP)[66,67] (as seen in Figure S2).

**Uptake Coefficient.** The kinetic behavior of the $NO_2$ can be described by assuming a pseudo-first-order reaction. The first-order rate constant ($k_{obs}$) is related to the geometric uptake coefficient ($\gamma_{geo}$) using eq 1:

$$\frac{d}{dt}\ln\frac{C_0}{C_i} = k_{obs} = \frac{\gamma_{geo}\langle c\rangle}{2r_{tube}} \quad (1)$$

where $r_{tube}$, $t$, and $\langle c\rangle$ are the flow tube radius, the exposure time, and the $NO_2$ average molecular velocity, respectively. $C_0$ and $C_i$ are the $NO_2$ concentrations at $t = 0$ and $t = i$, respectively.

If the loss of $NO_2$ at the particle surface is too rapid to be recovered with the $NO_2$ supply, a radial concentration gradient in the gas phase will be formed, which may cause diffusion limitations. Therefore, a correction for diffusion in the gas phase was taken into account using the Cooney−Kim−Davis (CKD) method.[68,69] Then, the true uptake coefficient ($\gamma_{BET}$) was obtained from the mass-dependence of $\gamma_{geo}$ using eq 2:[47,70]

$$\gamma_{BET} = \frac{S_{geo}}{S_{BET}} \times \text{slope} \quad (2)$$

where $S_{geo}$ is the inner surface area of the sample tube ($cm^2$), $S_{BET}$ is the specific surface area of the particle sample ($cm^2{\cdot}mg^{-1}$), and slope is the slope of the plot of $\gamma_{geo}$ versus sample mass in the linear regime ($mg^{-1}$).

**In Situ DRIFTS.** The heterogeneous reactions of $SO_2$ and $NO_2$ on MgO particles were measured by in situ diffuse reflectance Fourier transformed infrared spectroscopy (in situ DRIFTS, *is*50, Thermo Fisher Scientific), equipped with an in situ diffuse reflection chamber and a high-sensitivity mercury cadmium telluride (MCT) detector cooled by liquid $N_2$. Before the experiment, MgO particles were finely ground and placed into a ceramic crucible in the in situ chamber. The samples were first pretreated at 373 K for 120 min in a stream of synthetic air in a total flow of 100 $mL{\cdot}min^{-1}$. After the temperature was cooled to room temperature (295 K), the samples were exposed to reactant gases. The infrared spectra were collected using a computer with OMNIC 6.0 software (Nicolet Corporation). All spectra were recorded at a resolution of 4 $cm^{-1}$ for 100 scans in the spectral range of 600 to 4000 $cm^{-1}$, and then Kubelka−Munk (K−M) conversion was conducted. The low frequency cutoff of the spectra was due to the strong lattice oxide absorption of the samples.

**Ion Chromatograph Analysis.** Water-soluble inorganic anions were analyzed using an ion chromatograph (ICS-1000, Dionex Corporation), which consists of a guard column


DOI: 10.1021/acs.est.6b05724
Environ. Sci. Technol. 2017, 51, 3767−3775

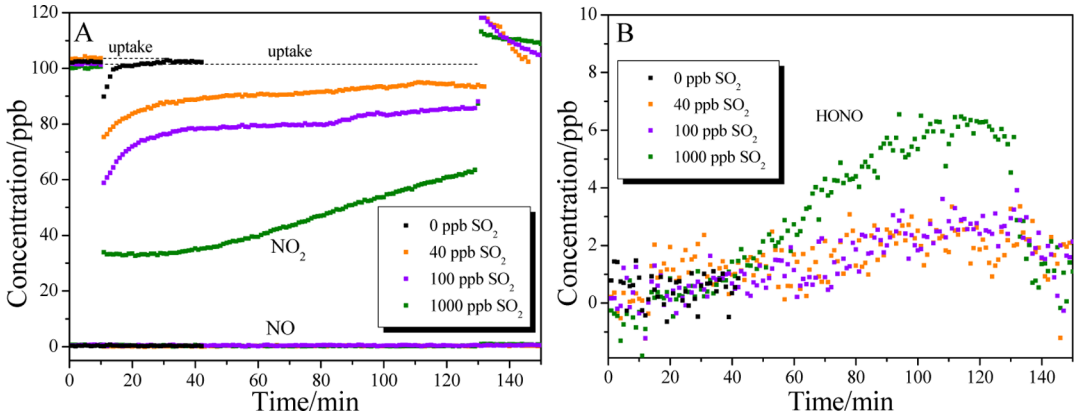


**Figure 1.** Comparison of $NO_2$ uptake on MgO in the presence of various $SO_2$ concentrations: 0 ppbv (177.42 mg, black), 40 ppbv (43.15 mg orange), 100 ppbv (33.47 mg, violet), and 1000 ppbv $SO_2$ (48.96 mg, olive). (A) $NO_2$ uptake and NO formation, (B) HONO formation. RH = 7.5%. Desorption of $NO_2$ occurred when the injector was pushed to the end of the flow tube after 120 min of reaction.

(AG14A) and an analytical column (AS14A). An electrolytic suppressor (ASRS 300 4 mm) was used to reduce the conductivity of the eluent. A concentrator (TAC-LP1) was installed. The analysis was performed by using 8 mM sodium carbonate and 1 mM sodium bicarbonate eluent at a flow rate of 0.6 mL $min^{-1}$. Multipoint calibrations were performed by using calibration standard solutions (Dionex Corporation, seven anion standards for anion). Good linearity of the calibration curve was obtained with $R^2 > 0.996$. The anions $NO_2^-$, $NO_3^-$, and $SO_4^{2-}$, were analyzed. $SO_3^{2-}$ was not analyzed because the column is not able to analyze $SO_3^{2-}$ ion.

## RESULTS AND DISCUSSION

**Effect of $SO_2$ on $NO_2$ Uptake.** Figure 1 shows $NO_2$ uptake on MgO particles in the presence of various $SO_2$ concentrations (0, 40, 100, and 1000 ppbv). When MgO was exposed to 100 ppbv $NO_2$ in the absence of $SO_2$, $NO_2$ concentrations decreased slightly and returned to the initial concentration in 10 min. This indicated the reaction of $NO_2$ on the fresh MgO surface is weak. In contrast, sharp decrease of $NO_2$ concentration was detected in all $NO_2$ uptake processes with the coexistence of $SO_2$. The uptake process lasted much more than 2 h, and the sample surfaces were quite beyond saturation. Blank experiment showed that no reaction between $NO_2$ and $SO_2$ on the quartz tube occurred under this reaction condition (as shown in Figure S3). Thus, this significant decrease of $NO_2$ concentration could be attributed to the uptake of $NO_2$ on MgO surface by coexisting $SO_2$. Increasing in $SO_2$ concentrations could increase the initial uptake coefficients as well as adsorption amounts of $NO_2$ on MgO, as seen in Figure 1A. This suggested $NO_2$ adsorption sites may relate to $SO_2$ adsorbed species on MgO surface.

For gaseous products, no NO was observed during all the uptake experiments, as can be seen in Figure 1A. This is in agreement with Liu et al., in which NO was not observed in the uptake of $NO_2$ on kaolin and hematite using coated-wall flow tube.[47] However, Underwood et al. observed NO as a predominant gas-phase product in the reaction of $NO_2$ with mineral oxides using Fourier transform infrared spectroscopy (FTIR) and Knudsen cell reactor.[71] This difference is likely due to the various reaction conditions, such as $NO_2$ concentration, relative humidity, pressure, and oxygen content in reactor.[31,47,62,71] For example, in Underwood et al., high $NO_2$ concentration was used, which favored a Langmuir–Hinshelwood (LH) or Eley–Rideal (ER) type mechanism of $NO_2$ and nitrite to produce NO and nitrate.[71] Moreover, both the FTIR and Knudsen cell reactors are under vacuum condition in which the RH and oxygen content were very low.[71] The $O_2$ (20% in volume) present in the flow tube reactor could inhibit the formation of NO.[31,47] In the present study, NO was not observed, which was mainly due to the low concentration of $NO_2$ and the synthetic air conditions. In addition, the coexisting $SO_2$ may also change the reaction mechanism of $NO_2$.

Unlike NO, HONO was observed as a product in all $NO_2$ uptake processes in the presence of $SO_2$, as seen in Figure 1B. The concentration of HONO increased gradually as the reaction proceeded. In previous studies, Liu et al. found HONO was formed in the uptake of $NO_2$ on kaolin and hematite.[47] However, in the present study, the formation of HONO was not obvious in the reaction between $NO_2$ and MgO without $SO_2$. This may be due to the low reactivity of MgO to $NO_2$, which limited the formation of HONO. These results suggested that $SO_2$ could change the reaction mechanism of $NO_2$ on MgO particles. The role of $SO_2$ on the uptake of $NO_2$ and the formation of HONO will be discussed later.

**Uptake Coefficients of $NO_2$.** The initial geometric uptake coefficients ($\gamma_{geo}$) of $NO_2$ on MgO surface under different reaction conditions were compared in Figure 2. The $SO_2$-aged MgO samples were prepared by exposing MgO particles to 1000 ppbv $SO_2$ in synthetic air for 12 h. As seen in Figure 2, $\gamma_{geo}$ of $NO_2$ on fresh MgO exhibited a linear mass effect, with a slope of $4.79 \times 10^{-8}$ $mg^{-1}$. This is due to the diffusion of $NO_2$ into underlying layers of the sample. The true uptake coefficients ($\gamma_{BET}$) were calculated using eq 2. $\gamma_{BET}$ of $NO_2$ on fresh MgO is about $2.44 \times 10^{-9}$, indicating weak reactivity of fresh MgO particles to $NO_2$. This value is lower than that measured by Underwood et al., in which they reported a true uptake coefficient of $1.2 \times 10^{-5}$. This discrepancy may be due to the different measurement methods. Underwood et al. used a Knudsen cell in which samples were under vacuum condition. In the flow tube reactor, $O_2$ and $H_2O$ in carrier gas may exhibit a competitive effect to $NO_2$ reaction and decreased the uptake coefficient of $NO_2$.[31,47]

The uptake coefficients obtained in $NO_2$ reaction on $SO_2$-aged MgO as well as in the reaction of $NO_2$ coexisting $SO_2$ are independent of sample mass in the mass range of 6–300 mg. A


DOI: 10.1021/acs.est.6b05724
Environ. Sci. Technol. 2017, 51, 3767–3775

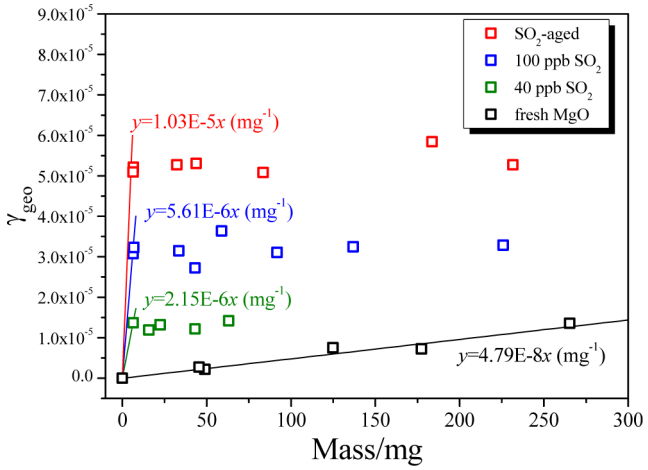


**Figure 2.** Mass dependence of initial geometric uptake coefficients ($\gamma_{geo}$) of 100 ppbv $NO_2$ on different MgO surfaces at 7.5% RH: fresh MgO (black), $SO_2$-aged MgO (red), and fresh MgO coexisting with 100 ppbv $SO_2$ (blue) and 40 ppbv $SO_2$ (olive).

further decrease in sample mass was not adopted because it is difficult to achieve complete coverage of the sample tubes. Because the diffusion of $NO_2$ or $SO_2$ into the underlying layers of powdered samples was found to readily occur, the BET surface area of the powdered samples was always used to calculate the true uptake coefficients.[61,62] Therefore, we estimated the $\gamma_{BET}$ based on the initial geometric uptake coefficients on sample with the minimum mass available. The true uptake coefficients of $NO_2$ were about $5.28 \times 10^{-6}$ for $SO_2$-aged MgO samples and about $2.87 \times 10^{-6}$ and $1.03 \times 10^{-6}$ for fresh MgO in the presence of 100 and 40 ppbv $SO_2$, respectively. It should be noted that these results should be considered as lower-limit values.

The mass-independent initial geometric uptake coefficients of $NO_2$ depend on the concentration of $SO_2$ or $SO_2$ aging process (as seen in Figure S4). When the concentration of $SO_2$ was above 1000 ppbv, the uptake coefficients of $NO_2$ reached a plateau and were close to that on $SO_2$-aged MgO. The saturation effect of $SO_2$ on uptake coefficients of $NO_2$ might be due to a Langmuir-type adsorption of $SO_2$ on MgO.[61] These results further indicated a close relation between adsorbed $SO_2$ species and $NO_2$ adsorption sites on MgO surface.

The effect of concentrations and relative humidity on $\gamma_{geo}$ of $NO_2$ on $SO_2$-aged MgO was compared in Figure 3. Values of $\gamma_{geo}$ were measured in mass-independent regime (10−15 mg). The error bars represent the standard deviation ($\sigma$) for three independent experiments. As seen in Figure 3A, the uptake coefficients of $NO_2$ were independent of the concentration of $NO_2$ in the range of 20−160 ppbv, indicating a first order reaction of $NO_2$ on $SO_2$-aged MgO. As for the humidity, increasing RH in the reactor had little influence on the initial geometric uptake coefficients of $NO_2$ on $SO_2$-aged MgO (Figure 3B). It should be noted that the increase of relative humidity has always exhibited negative effect on the uptake of $NO_2$ on fresh particles, which was explained by competitive adsorption between $NO_2$ and $H_2O$ on surface.[29,31,47] These results in our study indicated that the adsorption sites for $NO_2$ on $SO_2$-aged MgO may be not adsorbed water or surface species like reactive oxygen or hydroxyls. Instead, adsorbed $SO_2$ species should relate to $NO_2$ adsorption sites on MgO surface.

**Yield of HONO.** Formations of HONO were observed in all the $NO_2$ uptake experiments on MgO in the presence of $SO_2$. The effect of relative humidity on the yield of HONO in the uptake of $NO_2$ on $SO_2$-aged MgO was compared in Figure 4.

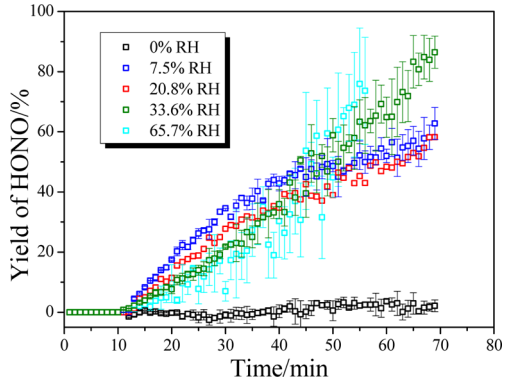


**Figure 4.** Effect of relative humidity on the yield of HONO on $SO_2$-aged MgO particles. (Sample mass: 10−15 mg).

The measured yields of HONO were calculated by the ratio of HONO formed to $NO_2$ consumed. There was little HONO formation under dry conditions, while the generation of HONO was detected under humid conditions. This indicated that surface $H_2O$ was necessary for the formation of HONO. However, the HONO yields were not influenced by RH. It should be noted that the $\gamma_{geo}$ of $NO_2$ on $SO_2$-aged MgO particles were also not influenced by RH (Figure 3B). These results suggested that surface $H_2O$ was not involved in the initial reaction step of $NO_2$ on $SO_2$-aged MgO. Instead, surface

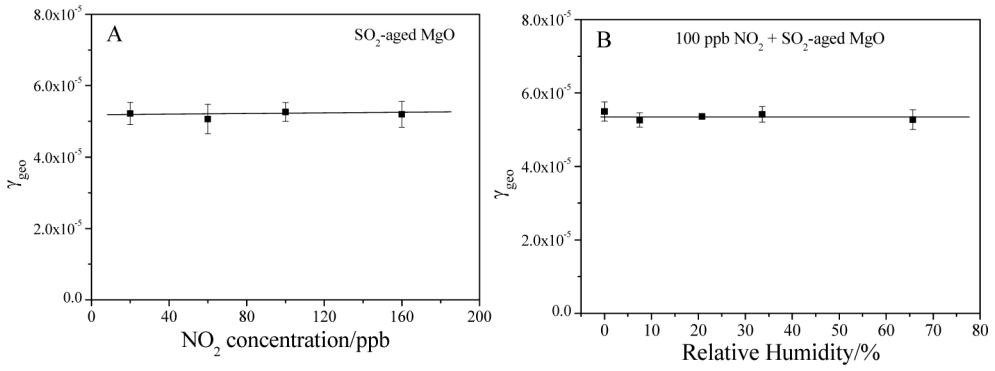


**Figure 3.** Effect of (A) $NO_2$ concentrations (RH = 7.5%) and (B) RH on the $\gamma_{geo}$ of $NO_2$ on $SO_2$-aged MgO particles. (Sample mass: 10−15 mg).



DOI: 10.1021/acs.est.6b05724
Environ. Sci. Technol. 2017, 51, 3767−3775

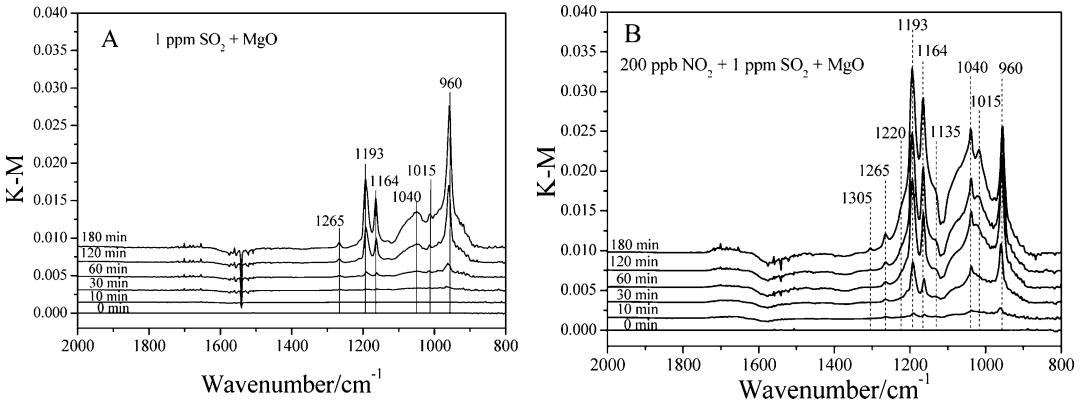


**Figure 5.** In situ DRIFTS spectra of MgO exposed to (A) 1000 ppbv $SO_2$ and (B) 1000 ppbv $SO_2$ and 200 ppbv $NO_2$ as a function of time. RH = 4.5%.

$H_2O$ reacted with the products of $NO_2$ reaction. Thus, the increase in RH may not increase the HONO yield.

In the presence of $H_2O$, the measured yields of HONO increased gradually as the reaction proceeded. The HONO yield beyond 50% was observed in the later stage of reaction, implying the formation of HONO maybe not through the hydrolysis reaction (disproportionation of $NO_2$ to equal HONO and $HNO_3$ with HONO yield less than 50%).[14,16] Constant HONO yield as well as steady state uptake of $NO_2$ was not observed, indicating that this reaction is not a catalytic reaction. The reaction mechanism will be discussed later.

Besides, the measured yields of HONO also depended on sample mass (as seen in Figure S5). The observed yields of HONO decreased with increasing MgO mass. Due to the alkalinity of MgO, the formed HONO may tend to adsorb on the surface as nitrite species instead of releasing to gas phase if the sample mass was large. Desorption of HONO was also observed when the uptake process was stopped (as seen in Figure 1B). Otherwise, when the sample mass was small, HONO yield beyond 100% could be observed when the consumption of $NO_2$ was close to zero; namely, the surface was almost saturated (as seen in Figure S6). This may be caused by the equilibrium between the surface nitrite and gas-phase HONO. Thus, the surface species should be further analyzed.

**Surface Products.** To study the dynamic change of surface species, in situ DRIFTS measurements was used to characterize the reaction of $NO_2$, $SO_2$, and $NO_2$ and $SO_2$ on MgO. The reactivity of MgO to 200 ppbv $NO_2$ was quite weak, and no obvious surface species were observed (as seen in Figure S7), which was in good agreement with the results of flow tube experiments (Figure 1). As shown in Figure 5A, the reaction of $SO_2$ (1000 ppbv) on MgO resulted in the formation of sulfite (960 $cm^{-1}$) and sulfate (1015, 1040, 1164, 1193, and 1265 $cm^{-1}$).[59,61] The sulfite was the dominant surface species in the individual $SO_2$ reaction, which was in consistent with previous studies.[59,61,63,72] In the reaction of $NO_2$ and $SO_2$ on MgO (Figure 5B), surface species including sulfite (960 $cm^{-1}$), sulfate (1265, 1193, 1164, 1135, 1040, and 1015 $cm^{-1}$), and nitrite (1305 and 1220 $cm^{-1}$)[73,74] were detected during the reaction. Compared to the individual $SO_2$ reaction (Figure 5A), the intensity of peak at 960 $cm^{-1}$ due to sulfite species decreased, while peaks at 1265, 1193, 1164, 1135, 1040, and 1015 $cm^{-1}$ (corresponding to sulfate) increased. These results suggested that the presence of $NO_2$ could enhance the conversion of $SO_2$ to sulfate.

For surface nitrogen-containing species, only surface nitrite (1305 and 1220 $cm^{-1}$) was observed. No peaks attributed to surface nitrate species (typically in the range of 1500−1650 $cm^{-1}$) was observed.[59,71] These results indicated that $SO_2$ was oxidized to sulfate, while $NO_2$ was reduced to nitrite in the reaction between $NO_2$ and $SO_2$ on MgO surface, implying this was a redox reaction. The surface products were also confirmed by ion chromatography (IC) analysis (as seen in Figure S8). The main water-soluble ions were detected to be sulfate and nitrite with little nitrate. Thus, the final products of $NO_2$ reaction on MgO in the presence of $SO_2$ were HONO and nitrite, combined the results of flow tube and DRIFTS experiments. Considering the convertibility between HONO and nitrite, the yields of HONO (HONO and nitrite) in the present study could be regarded as 100%.

**Proposed Reaction Mechanism.** As shown above, the coexisting $SO_2$ was determined to enhance the uptake of $NO_2$ on MgO and the transformation to HONO and nitrite. This means $SO_2$ could change the reaction mechanism of $NO_2$ on MgO. There are several proposed mechanisms of $NO_2$ adsorption on mineral oxides in previous researches. For example, Underwood et al.[71] suggested a two-step mechanism in which gas-phase $NO_2$ is initially adsorbed as a nitrite species that subsequently reacts with another nitrite (Langmuir−Hinshelwood type) or additional $NO_2$ (Eley−Rideal type) to form surface nitrate and gas-phase NO. This mechanism of $NO_2$ adsorption on mineral oxide surface may be mainly due to the high $NO_2$ concentration used. In the present study, much lower $NO_2$ concentration was used. In addition, neither gaseous NO nor surface nitrate species were observed. Thus, this mechanism was excluded from our results.

Previous studies also proposed that the hydrolysis of $NO_2$ on wet surfaces results in the generation of gaseous HONO and surface $HNO_3$.[16−18,47,75] When $NO_2$ was in high concentration level, dimerization of gaseous $NO_2$ led to the formation of $N_2O_4$ intermediate, which then reacted with $H_2O$ to form HONO and $HNO_3$.[17,18] In the hydrolysis reaction of $NO_2$ with low concentration, it was proposed that dissociative chemisorption of $H_2O$ to yield $H_{ads}$ and $OH_{ads}$ on the surface, which further reacted with $NO_2$ to form HONO and $HNO_3$.[47,75] The yield of HONO should be less than 50% through this disproportionation reaction. Much higher yields than 50% were obtained in this work, however, indicating that the HONO formation on $SO_2$-aged MgO could not be attributed to hydrolysis reaction.



DOI: 10.1021/acs.est.6b05724
Environ. Sci. Technol. 2017, 51, 3767−3775

Recently, Kebede et al. demonstrated the formation of HONO in the redox reactions between $NO_2$ and $Fe^{2+}$(aq) present in water films on the surface of iron-bearing minerals.[13] The yield of HONO could be larger than 50% when $NO_2$ underwent a redox reaction on surfaces.[13,47] However, unlike Fe, Mg is not a valence-varied metal. This could explain no HONO formation in the uptake of $NO_2$ on MgO without $SO_2$. Therefore, the conversion of $NO_2$ to HONO on MgO in the presence of $SO_2$ may be due to the redox reaction between $NO_2$ and surface sulfur-containing species.

It is well-known that adsorption of $SO_2$ on mineral particles leads to the formation of surface sulfite species, while additional oxidants like $O_3$ and $NO_2$ were needed to oxidize sulfite to sulfate.[58,63,72] Although both sulfite and sulfate were observed during the adsorption of $SO_2$ on MgO, sulfite was the main surface species on MgO.[59,61] In the present study, to confirm the role of surface sulfite species on the uptake of $NO_2$, $SO_2$-aged MgO samples were further exposed to 500 ppbv $O_3$ for forcing oxidation of sulfite to sulfate. $NO_2$ uptake decreased greatly on these samples (seen in Figure S9), indicating surface sulfite species were the reducing agent for the conversion of $NO_2$ to nitrite and HONO on MgO.

Therefore, we proposed a reaction mechanism of $NO_2$ on MgO in the presence of $SO_2$, as seen in Scheme 1. First, initial

**Scheme 1. Proposed Reaction Mechanism of $NO_2$ Adsorption on MgO in the Presence of $SO_2$**

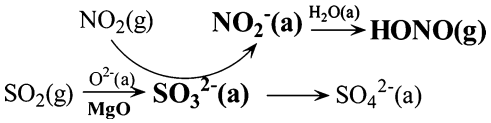


adsorption of $SO_2$ on MgO surface led to the formation of surface sulfite species ($SO_3^{2-}$), in which surface oxygen species ($O^{2-}$) was involved. These surface sulfite species then provided reactive sites for $NO_2$ adsorption. A redox reaction between $NO_2$ and sulfite occurred under dry condition and led to the formation of nitrite and sulfate species. If surface $H_2O$ was present, HONO was produced through the conversion of nitrite by $H_2O$.

Recently, Liu et al. found that coexisting $NO_2$ could enhance the conversion of $SO_2$ to sulfate on typical mineral oxides, in which $N_2O_4$ was observed as an intermediate and nitrate was the final nitrogen-containing product on surfaces.[59] In the present study, the presence of $SO_2$ initiated the conversion of $NO_2$ to nitrite on MgO, and nitrate was not observed. This discrepancy may be due to the high concentration of $NO_2$ (100 ppm) used in Liu et al.,[59] which was prone to the dimerization of $NO_2$ and can favor the conversion of nitrite to nitrate through an Eley–Rideal (ER) type mechanism.[71] When $NO_2$ concentration is in ppbv level (e.g., 100–200 ppbv in the present study), excess $SO_2$ could completely reduce $NO_2$ to HONO and nitrite on MgO surface. Therefore, nitrate species were not formed on the surface.

## ATMOSPHERIC IMPLICATIONS

Although HONO has been widely investigated in laboratory studies and field measurements, its sources are still not fully understood.[9,12,15,35] Here, we suggest a new potential formation pathway of HONO in polluted environments with high concentration of $SO_2$. The coexisting $SO_2$ was found to increase the true uptake coefficients of $NO_2$ on MgO by 2–3 orders of magnitude. Mg is the seventh most abundant element in Earth's crust, making it a major component of soil and windblown mineral dust.[40] Thus, this reaction could happen on both mineral dust and the ground surface, which could contribute to HONO sources in polluted region with high concentration of $SO_2$.

First, this redox reaction mechanism may help explain the high HONO concentrations observed in dust storms. Mineral particles account for a large fraction of global emissions of aerosol particles and can undergo long-range transport.[40,41] Mineral dust can encounter $SO_2$ during the transport, which could form sulfite on particle surfaces.[63,72] These $SO_2$-aged mineral particles could provide reactive sites for the conversion of $NO_2$ to HONO. For example, the observations of high correlation between HONO and sulfate in dusty days[48] might be partially due to the redox reaction between $SO_2$ and $NO_2$ on mineral particles. Nie et al.[76] recently reported observational evidence on new particle formation and growth in the remote ambient atmosphere during heavy dust episodes mixed with anthropogenic pollution and attributed photoinduced heterogeneous reactions of $NO_2$ to the source of HONO and OH. Considering the high concentrations of mineral particles, $SO_2$, and $NO_2$ observed in these dust events, the reaction between $SO_2$ and $NO_2$ on mineral particles could also contribute to the source of HONO.

Second, the redox reaction between $SO_2$ and $NO_2$ on surfaces may contribute to the formation of HONO in the haze episodes in China because high $SO_2$ concentration was always observed in the haze episodes. Haze in China has been increasing in frequency of occurrence as well as the area of the affected region, especially in the wintertime in the North China plain.[60] High concentrations of HONO were observed in the severe haze period in Beijing.[38,39] As demonstrated in the present study, the true uptake coefficient of $NO_2$ on MgO in the presence of $SO_2$ could be in the range of $1.0–5.2 \times 10^{-6}$, with a yield of HONO and nitrite about 100%. If a constant surface area to volume ratio ($S/V$) value of 0.3 $m^{-1}$ for ground surface was used,[77,78] HONO formation rates could be 0.18–0.96% $h^{-1}$ with an average loading (1.7%) of MgO in soil in north China (see detail in the Supporting Information). If the upper limit $\gamma$ (mass-independent uptake coefficients) was considered, the formation rate would further increase. However, mineral dust is also a major component (~35% in mass) of aerosol in the North China plain.[40,43] A recent study reported that the concentrations of $PM_{2.5}$ and $NO_2$ in a heavy haze episode could reach 228–545 $\mu g\ m^{-3}$ and 20–80 ppbv, respectively.[38] According to the average ratio of $PM_{2.5}/PM_{10}$ (0.5) during haze-fog episodes[79] and a surface area to volume ratio measured in Beijing,[80] the formation rate of HONO via the redox reaction of $NO_2$ and $SO_2$ on MgO in mineral dust is estimated to be 0.43–21.2 pptv $h^{-1}$ (see detail in the Supporting Information). Considering that the $S/V$ value of aerosol (<0.01 $m^{-1}$) is much lower than that of ground surface (~0.3 $m^{-1}$), the redox reaction between $SO_2$ and $NO_2$ on surfaces as a relevant HONO source will be more important on ground than on aerosol, even in the severe haze episodes in China. Accordingly, coexisting gases, especially $SO_2$, should be considered in future study of $NO_2$ conversion to HONO.

## ASSOCIATED CONTENT

### Supporting Information

The Supporting Information is available free of charge on the ACS Publications website at DOI: 10.1021/acs.est.6b05724.



DOI: 10.1021/acs.est.6b05724
Environ. Sci. Technol. 2017, 51, 3767–3775

Additional information about the diagram of coated-wall flow tube, the description of LOPAP and comparative measurement of HONO by LOPAP and two NO*x* analyzers, blank tube experiment, effect of $SO_2$ concentration on the uptake coefficients, mass effect on yield, the measured yields of HONO in the uptake of $NO_2$ on 8.08 mg $SO_2$-aged MgO, DRIFTS spectra of MgO exposed to 200 ppb $NO_2$, description of IC and measurement, and uptake experiment on $O_3$−$SO_2$-aged MgO and the description of the calculation of HONO formation rates. (PDF)

## AUTHOR INFORMATION


### Corresponding Authors

*Tel: +86 852 27666059; fax: +86 852 23346389; e-mail: qxma@rcees.ac.cn.

*E-mail: cetwang@polyu.edu.hk.

### ORCID

Qingxin Ma: 0000-0002-9668-7008


### Notes

The authors declare no competing financial interest.

## ACKNOWLEDGMENTS

This work was supported by the Collaborative Research Fund of the Hong Kong Research Grants Council (C5022-14G), the National Natural Science Foundation of China (41305116), PolyU Project of Strategic Importance (1-ZE13), and the "Strategic Priority Research Program" of the Chinese Academy of Sciences (XDB05040401 and XDB05010300). We are thankful for the support of the Hong Kong Scholar program. We are grateful of the suggestions from Dr. Christian George and appreciate the suggestions from all reviewers.

## REFERENCES


(1) Harrison, R. M.; Peak, J. D.; Collins, G. M. Tropospheric cycle of nitrous acid. *J. Geophys. Res.* **1996**, *101* (D9), 14429−14439.

(2) Kleffmann, J.; Lörzer, J. C.; Wiesen, P.; Kern, C.; Trick, S.; Volkamer, R.; Rodenas, M.; Wirtz, K. Intercomparison of the DOAS and LOPAP techniques for the detection of nitrous acid (HONO). *Atmos. Environ.* **2006**, *40* (20), 3640−3652.

(3) Kleffmann, J. Daytime sources of nitrous acid (HONO) in the atmospheric boundary layer. *ChemPhysChem* **2007**, *8* (8), 1137−1144.

(4) Elshorbany, Y. F.; Kurtenbach, R.; Wiesen, P.; Lissi, E.; Rubio, M.; Villena, G.; Gramsch, E.; Rickard, A. R.; Pilling, M. J.; Kleffmann, J. Oxidation capacity of the city air of Santiago, Chile. *Atmos. Chem. Phys.* **2009**, *9* (6), 2257−2273.

(5) Pitts, J. N.; Grosjean, D.; Van Cauwenberghe, K.; Schmid, J. P.; Fitz, D. R. Photooxidation of aliphatic amines under simulated atmospheric conditions: formation of nitrosamines, nitramines, amides, and photochemical oxidant. *Environ. Sci. Technol.* **1978**, *12* (8), 946−953.

(6) Gligorovski, S. Nitrous acid (HONO): An emerging indoor pollutant. *J. Photochem. Photobiol., A* **2016**, *314*, 1−5.

(7) Su, H.; Cheng, Y.; Oswald, R.; Behrendt, T.; Trebs, I.; Meixner, F. X.; Andreae, M. O.; Cheng, P.; Zhang, Y.; Pöschl, U. Soil nitrite as a source of atmospheric HONO and OH radicals. *Science* **2011**, *333* (6049), 1616−1618.

(8) Li, X.; Brauers, T.; Häseler, R.; Bohn, B.; Fuchs, H.; Hofzumahaus, A.; Holland, F.; Lou, S.; Lu, K. D.; Rohrer, F.; Hu, M.; Zeng, L. M.; Zhang, Y. H.; Garland, R. M.; Su, H.; Nowak, A.; Wiedensohler, A.; Takegawa, N.; Shao, M.; Wahner, A. Exploring the atmospheric chemistry of nitrous acid (HONO) at a rural site in Southern China. *Atmos. Chem. Phys.* **2012**, *12* (3), 1497−1513.

(9) Spataro, F.; Ianniello, A. Sources of atmospheric nitrous acid: State of the science, current research needs, and future prospects. *J. Air Waste Manage. Assoc.* **2014**, *64* (11), 1232−1250.

(10) George, C.; Ammann, M.; D'Anna, B.; Donaldson, D. J.; Nizkorodov, S. A. Heterogeneous photochemistry in the atmosphere. *Chem. Rev.* **2015**, *115* (10), 4218−4258.

(11) Monge, M. E.; D'Anna, B.; Mazri, L.; Giroir-Fendler, A.; Ammann, M.; Donaldson, D. J.; George, C. Light changes the atmospheric reactivity of soot. *Proc. Natl. Acad. Sci. U. S. A.* **2010**, *107* (15), 6605−6609.

(12) Indarto, A. Heterogeneous reactions of HONO formation from $NO_2$ and $HNO_3$: a review. *Res. Chem. Intermed.* **2012**, *38* (3), 1029−1041.

(13) Kebede, M. A.; Bish, D. L.; Losovyj, Y.; Engelhard, M. H.; Raff, J. D. The Role of Iron-Bearing Minerals in $NO_2$ to HONO Conversion on Soil Surfaces. *Environ. Sci. Technol.* **2016**, *50* (16), 8649−8660.

(14) Finlayson-Pitts, B. J.; Wingen, L. M.; Sumner, A. L.; Syomin, D.; Ramazan, K. A. The heterogeneous hydrolysis of $NO_2$ in laboratory systems and in outdoor and indoor atmospheres: An integrated mechanism. *Phys. Chem. Chem. Phys.* **2003**, *5* (2), 223−242.

(15) Ma, J.; Liu, Y.; Han, C.; Ma, Q.; Liu, C.; He, H. Review of heterogeneous photochemical reactions of NOy on aerosol—A possible daytime source of nitrous acid (HONO) in the atmosphere. *J. Environ. Sci.* **2013**, *25* (2), 326−334.

(16) Kleffmann, J.; Becker, K. H.; Wiesen, P. Heterogeneous $NO_2$ conversion processes on acid surfaces: possible atmospheric implications. *Atmos. Environ.* **1998**, *32* (16), 2721−2729.

(17) Goodman, A. L.; Underwood, G. M.; Grassian, V. H. Heterogeneous Reaction of $NO_2$: Characterization of Gas-Phase and Adsorbed Products from the Reaction, $2NO_2(g) + H_2O(a) \rightarrow HONO(g) + HNO_3(a)$ on Hydrated Silica Particles. *J. Phys. Chem. A* **1999**, *103* (36), 7217−7223.

(18) Barney, W. S.; Finlayson-Pitts, B. J. Enhancement of $N_2O_4$ on porous glass at room temperature: A key intermediate in the heterogeneous hydrolysis of $NO_2$? *J. Phys. Chem. A* **2000**, *104* (2), 171−175.

(19) Ammann, M.; Kalberer, M.; Jost, D. T.; Tobler, L.; Rössler, E.; Piguet, D.; Gäggeler, H. W.; Baltensperger, U. Heterogeneous production of nitrous acid on soot in polluted air masses. *Nature* **1998**, *395* (6698), 157−160.

(20) Arens, F.; Gutzwiller, L.; Baltensperger, U.; Gäggeler, H. W.; Ammann, M. Heterogeneous reaction of $NO_2$ on diesel soot particles. *Environ. Sci. Technol.* **2001**, *35* (11), 2191−2199.

(21) Kleffmann, J.; Becker, K. H.; Lackhoff, M.; Wiesen, P. Heterogeneous conversion of $NO_2$ on carbonaceous surfaces. *Phys. Chem. Chem. Phys.* **1999**, *1*, 5443−5450.

(22) Aubin, D. G.; Abbatt, J. P. Interaction of $NO_2$ with hydrocarbon soot: Focus on HONO yield, surface modification, and mechanism. *J. Phys. Chem. A* **2007**, *111* (28), 6263−6273.

(23) Han, C.; Liu, Y.; He, H. Role of organic carbon in heterogeneous reaction of $NO_2$ with soot. *Environ. Sci. Technol.* **2013**, *47* (7), 3174−3181.

(24) Stemmler, K.; Ammann, M.; Donders, C.; Kleffmann, J.; George, C. Photosensitized reduction of nitrogen dioxide on humic acid as a source of nitrous acid. *Nature* **2006**, *440*, 195−198.

(25) Han, C.; Yang, W.; Wu, Q.; Yang, H.; Xue, X. Heterogeneous Photochemical Conversion of $NO_2$ to HONO on the Humic Acid Surface under Simulated Sunlight. *Environ. Sci. Technol.* **2016**, *50* (10), 5017−5023.

(26) Stemmler, K.; Ndour, M.; Elshorbany, Y.; Kleffmann, J.; D'anna, B.; George, C.; Bohn, B.; Ammann, M. Light induced conversion of nitrogen dioxide into nitrous acid on submicron humic acid aerosol. *Atmos. Chem. Phys.* **2007**, *7* (16), 4237−4248.

(27) George, C.; Strekowski, R. S.; Kleffmann, J.; Stemmler, K.; Ammann, M. Photoenhanced uptake of gaseous $NO_2$ on solid organic compounds: a photochemical source of HONO? *Faraday Discuss.* **2005**, *130*, 195−210.




DOI: 10.1021/acs.est.6b05724
*Environ. Sci. Technol.* 2017, 51, 3767−3775

(28) Brigante, M.; Cazoir, D.; D'Anna, B.; George, C.; Donaldson, D. J. Photoenhanced Uptake of $NO_2$ by Pyrene Solid Films. *J. Phys. Chem. A* **2008**, *112* (39), 9503−9508.
(29) Gustafsson, R. J.; Orlov, A.; Griffiths, P. T.; Cox, R. A.; Lambert, R. M. Reduction of $NO_2$ to nitrous acid on illuminated titanium dioxide aerosol surfaces: implications for photocatalysis and atmospheric chemistry. *Chem. Commun.* **2006**, *37*, 3936−3938.
(30) Ndour, M.; D'Anna, B.; George, C.; Ka, O.; Balkanski, Y.; Kleffmann, J.; Stemmler, K.; Ammann, M. Photoenhanced uptake of $NO_2$ on mineral dust: Laboratory experiments and model simulations. *Geophys. Res. Lett.* **2008**, *35* (5), L05812.
(31) Monge, M. E.; D'Anna, B.; George, C. Nitrogen dioxide removal and nitrous acid formation on titanium oxide surfaces—an air quality remediation process? *Phys. Chem. Chem. Phys.* **2010**, *12* (31), 8991−8998.
(32) Ndour, M.; Nicolas, M.; D'Anna, B.; Ka, O.; George, C. Photoreactivity of $NO_2$ on mineral dusts originating from different locations of the Sahara desert. *Phys. Chem. Chem. Phys.* **2009**, *11* (9), 1312−1319.
(33) Kleffmann, J.; Kurtenbach, R.; Lörzer, J.; Wiesen, P.; Kalthoff, N.; Vogel, B.; Vogel, H. Measured and simulated vertical profiles of nitrous acid—Part I: Field measurements. *Atmos. Environ.* **2003**, *37* (21), 2949−2955.
(34) Wong, K. W.; Tsai, C.; Lefer, B.; Haman, C.; Grossberg, N.; Brune, W. H.; Ren, X.; Luke, W.; Stutz, J. Daytime HONO vertical gradients during SHARP 2009 in Houston, TX. *Atmos. Chem. Phys.* **2012**, *12* (2), 635−652.
(35) VandenBoer, T. C.; Brown, S. S.; Murphy, J. G.; Keene, W. C.; Young, C. J.; Pszenny, A. A. P.; Kim, S.; Warneke, C.; de Gouw, J. A.; Maben, J. R.; Wagner, N. L.; Riedel, T. P.; Thornton, J. A.; Wolfe, D. E.; Dubé, W. P.; Öztürk, F.; Brock, C. A.; Grossberg, N.; Lefer, B.; Lerner, B.; Middlebrook, A. M.; Roberts, J. M. Understanding the role of the ground surface in HONO vertical structure: High resolution vertical profiles during NACHTT-11. *J. Geophys. Res.* **2013**, *118*, 10155−10171.
(36) An, J.; Li, Y.; Chen, Y.; Li, J.; Qu, Y.; Tang, Y. Enhancements of major aerosol components due to additional HONO sources in the North China Plain and implications for visibility and haze. *Adv. Atmos. Sci.* **2013**, *30* (1), 57−66.
(37) Liu, Z.; Wang, Y.; Costabile, F.; Amoroso, A.; Zhao, C.; Huey, L. G.; Stickel, R.; Liao, J.; Zhu, T. Evidence of aerosols as a media for rapid daytime HONO production over China. *Environ. Sci. Technol.* **2014**, *48* (24), 14386−14391.
(38) Hou, S.; Tong, S.; Ge, M.; An, J. Comparison of atmospheric nitrous acid during severe haze and clean periods in Beijing, China. *Atmos. Environ.* **2016**, *124*, 199−206.
(39) Tong, S.; Hou, S.; Zhang, Y.; Chu, B.; Liu, Y.; He, H.; Zhao, P.; Ge, M. Exploring the nitrous acid (HONO) formation mechanism in winter Beijing: direct emissions and heterogeneous production in urban and suburban areas. *Faraday Discuss.* **2016**, *189*, 213−230.
(40) Usher, C. R.; Michel, A. E.; Grassian, V. H. Reactions on mineral dust. *Chem. Rev.* **2003**, *103* (12), 4883−4940.
(41) Gieré, R.; Querol, X. Solid Particulate Matter in the Atmosphere. *Elements* **2010**, *6* (4), 215−222.
(42) Zhang, X. Y.; Gong, S. L.; Shen, Z. X.; Mei, F. M.; Xi, X. X.; Liu, L. C.; Zhou, Z. J.; Wang, D.; Wang, Y. Q.; Cheng, Y. Characterization of soil dust aerosol in China and its transport and distribution during 2001 ACE-Asia 1. Network observations. *J. Geophys. Res.* **2003**, *108* (D9), 8032−8039.
(43) Zhang, X. Y.; Wang, Y. Q.; Niu, T.; Zhang, X. C.; Gong, S. L.; Zhang, Y. M.; Sun, J. Y. Atmospheric aerosol compositions in China: spatial/temporal variability, chemical signature, regional haze distribution and comparisons with global aerosols. *Atmos. Chem. Phys.* **2012**, *12* (2), 779−799.
(44) Tegen, I.; Fung, I. Modeling of mineral dust in the atmosphere: Sources, transport, and optical thickness. *J. Geophys. Res.* **1994**, *99* (D11), 22897−22914.
(45) Wang, S.; Ackermann, R.; Spicer, C. W.; Fast, J. D.; Schmeling, M.; Stutz, J. Atmospheric observations of enhanced $NO_2$-HONO conversion on mineral dust particles. *Geophys. Res. Lett.* **2003**, *30* (11), 1595.
(46) Crowley, J. N.; Ammann, M.; Cox, R. A.; Hynes, R. G.; Jenkin, M. E.; Mellouki, A.; Rossi, M. J.; Troe, J.; Wallington, T. J. Evaluated kinetic and photochemical data for atmospheric chemistry: Volume V−heterogeneous reactions on solid substrates. *Atmos. Chem. Phys.* **2010**, *10* (18), 9059−9223.
(47) Liu, Y.; Han, C.; Ma, J.; Bao, X.; He, H. Influence of relative humidity on heterogeneous kinetics of $NO_2$ on kaolin and hematite. *Phys. Chem. Chem. Phys.* **2015**, *17* (29), 19424−19431.
(48) Saliba, N. A.; Moussa, S. G.; El Tayyar, G. Contribution of airborne dust particles to HONO sources. *Atmos. Chem. Phys. Discuss.* **2014**, *14* (4), 4827−4839.
(49) Wang, G.; Zhang, R.; Gomez, M. E.; Yang, L.; Zamora, M. L.; Hu, M.; Lin, Y.; Peng, J.; Guo, S.; Meng, J. Persistent sulfate formation from London Fog to Chinese haze. *Proc. Natl. Acad. Sci. U. S. A.* **2016**, *113* (48), 13630−13635.
(50) Xue, J.; Yuan, Z.; Griffith, S. M.; Yu, X.; Lau, A. K.; Yu, J. Z. Sulfate formation enhanced by a cocktail of high NOx, SO2, particulate matter and droplet pH during haze-fog events in megacities in China: An Observation-Based Modeling investigation. *Environ. Sci. Technol.* **2016**, *50* (14), 7325−7334.
(51) Lee, Y. N.; Schwartz, S. E. Kinetics of oxidation of aqueous sulfur (IV) by nitrogen dioxide. In *Precipitation Scavenging, Dry Deposition and Resuspension*, Vol *1*; Pruppacher, H. R., et al.; Elsevier: New York, NY, 1983.
(52) Martin, L. R.; Damschen, D. E.; Judeikis, H. S. The reactions of nitrogen oxides with $SO_2$ in aqueous aerosols. *Atmos. Environ.* **1981**, *15* (2), 191−195.
(53) Littlejohn, D.; Wang, Y.; Chang, S. G. Oxidation of aqueous sulfite ion by nitrogen dioxide. *Environ. Sci. Technol.* **1993**, *27* (10), 2162−2167.
(54) Shen, C. H.; Rochelle, G. T. Nitrogen dioxide absorption and sulfite oxidation in aqueous sulfite. *Environ. Sci. Technol.* **1998**, *32* (13), 1994−2003.
(55) Cofer, W. R.; Schryer, D. R.; Rogowski, R. S. Oxidation of $SO_2$ by $NO_2$ and $O_3$ on carbon: implications to tropospheric chemistry. *Atmos. Environ.* **1984**, *18* (1), 243−245.
(56) De Santis, F.; Allegrini, I. Heterogeneous reactions of $SO_2$ and $NO_2$ on carbonaceous surfaces. *Atmos. Environ., Part A* **1992**, *26* (16), 3061−3064.
(57) Ishizuka, T.; Kabashima, H.; Yamaguchi, T.; Tanabe, K.; Hattori, H. Initial Step of Flue Gas Desulfurization An IR Study of the Reaction of $SO_2$ with NO*x* on CaO. *Environ. Sci. Technol.* **2000**, *34* (13), 2799−2803.
(58) Ma, Q.; Liu, Y.; He, H. Synergistic effect between $NO_2$ and $SO_2$ in their adsorption and reaction on γ-Alumina. *J. Phys. Chem. A* **2008**, *112* (29), 6630−6635.
(59) Liu, C.; Ma, Q.; Liu, Y.; Ma, J.; He, H. Synergistic reaction between $SO_2$ and $NO_2$ on mineral oxides: a potential formation pathway of sulfate aerosol. *Phys. Chem. Chem. Phys.* **2012**, *14* (5), 1668−1676.
(60) He, H.; Wang, Y.; Ma, Q.; Ma, J.; Chu, B.; Ji, D.; Tang, G.; Liu, C.; Zhang, H.; Hao, J. Mineral dust and NOx promote the conversion of $SO_2$ to sulfate in heavy pollution days. *Sci. Rep.* **2014**, *4*, 4172.
(61) Goodman, A. L.; Li, P.; Usher, C. R.; Grassian, V. H. Heterogeneous uptake of sulfur dioxide on aluminum and magnesium oxide particles. *J. Phys. Chem. A* **2001**, *105* (25), 6109−6120.
(62) Underwood, G. M.; Song, C. H.; Phadnis, M.; Carmichael, G. R.; Grassian, V. H. Heterogeneous reactions of $NO_2$ and $HNO_3$ on oxides and mineral dust: A combined laboratory and modeling study. *J. Geophys. Res.* **2001**, *106* (D16), 18055−18066.
(63) Usher, C. R.; Al-Hosney, H.; Carlos-Cuellar, S.; Grassian, V. H. A laboratory study of the heterogeneous uptake and oxidation of sulfur dioxide on mineral dust particles. *J. Geophys. Res.* **2002**, *107* (D23), 4713.
(64) Zhang, X.; Zhuang, G.; Chen, J.; Wang, Y.; Wang, X.; An, Z.; Zhang, P. Heterogeneous reactions of sulfur dioxide on typical mineral particles. *J. Phys. Chem. B* **2006**, *110* (25), 12588−12596.


DOI: 10.1021/acs.est.6b05724
*Environ. Sci. Technol.* 2017, 51, 3767−3775

(65) Xu, Z.; Wang, T.; Xue, L. K.; Louie, P. K. K.; Luk, C. W. Y.; Gao, J.; Wang, S. L.; Chai, F. H.; Wang, W. X. Evaluating the uncertainties of thermal catalytic conversion in measuring atmospheric nitrogen dioxide at four differently polluted sites in China. *Atmos. Environ.* **2013**, *76*, 221−226.
(66) Heland, J.; Kleffmann, J.; Kurtenbach, R.; Wiesen, P. A new instrument to measure gaseous nitrous acid (HONO) in the atmosphere. *Environ. Sci. Technol.* **2001**, *35* (15), 3207−3212.
(67) Xu, Z.; Wang, T.; Wu, J.; Xue, L.; Chan, J.; Zha, Q.; Zhou, S.; Louie, P. K.; Luk, C. W. Nitrous acid (HONO) in a polluted subtropical atmosphere: Seasonal variability, direct vehicle emissions and heterogeneous production at ground surface. *Atmos. Environ.* **2015**, *106*, 100−109.
(68) Cooney, D. O.; Kim, S.-S.; Davis, E. J. Analyses of mass transfer in hemodialyzers for laminar blood flow and homogeneous dialysate. *Chem. Eng. Sci.* **1974**, *29* (8), 1731−1738.
(69) Murphy, D. M.; Fahey, D. W. Mathematical treatment of the wall loss of a trace species in denuder and catalytic converter tubes. *Anal. Chem.* **1987**, *59* (23), 2753−2759.
(70) Underwood, G. M.; Li, P.; Usher, C. R.; Grassian, V. H. Determining accurate kinetic parameters of potentially important heterogeneous atmospheric reactions on solid particle surfaces with a Knudsen cell reactor. *J. Phys. Chem. A* **2000**, *104* (4), 819−829.
(71) Underwood, G. M.; Miller, T. M.; Grassian, V. H. Transmission FT-IR and Knudsen cell study of the heterogeneous reactivity of gaseous nitrogen dioxide on mineral oxide particles. *J. Phys. Chem. A* **1999**, *103* (31), 6184−6190.
(72) Ullerstam, M.; Vogt, R.; Langer, S.; Ljungstrom, E. The kinetics and mechanism of $SO_2$ oxidation by $O_3$ on mineral dust. *Phys. Chem. Chem. Phys.* **2002**, *4* (19), 4694−4699.
(73) Cerruti, L.; Modone, E.; Guglielminotti, E.; Borello, E. Infra-red study of nitric oxide adsorption on magnesium oxide. *J. Chem. Soc., Faraday Trans. 1* **1974**, *70*, 729−739.
(74) Giamello, E.; Garrone, E.; Guglielminotti, E.; Zecchina, A. Nitric oxide adsorption onto NiO/MgO and CoO/MgO solid solutions: an IR and ESR study. *J. Mol. Catal.* **1984**, *24* (1), 59−69.
(75) Gustafsson, R. J.; Kyriakou, G.; Lambert, R. M. The molecular mechanism of tropospheric nitrous acid production on mineral dust surfaces. *ChemPhysChem* **2008**, *9* (10), 1390−1393.
(76) Nie, W.; Ding, A.; Wang, T.; Kerminen, V.-M.; George, C.; Xue, L.; Wang, W.; Zhang, Q.; Petäjä, T.; Qi, X.; et al. Polluted dust promotes new particle formation and growth. *Sci. Rep.* **2014**, *4*, 6634.
(77) Sarwar, G.; Roselle, S. J.; Mathur, R.; Appel, W.; Dennis, R. L.; Vogel, B. A comparison of CMAQ HONO predictions with observations from the Northeast Oxidant and Particle Study. *Atmos. Environ.* **2008**, *42* (23), 5760−5770.
(78) Zhang, L.; Wang, T.; Zhang, Q.; Zheng, J.; Xu, Z.; Lv, M. Potential Sources of Nitrous Acid (HONO) and Their Impacts on Ozone: A WRF-Chem study in a Polluted Subtropical Region. *J. Geophys. Res.* **2016**, *121*, 3645−3662.
(79) Sun, Y.; Zhuang, G.; Tang, A.; Wang, Y.; An, Z. An, Z. Chemical characteristics of $PM_{2.5}$ and $PM_{10}$ in haze-fog episodes in Beijing. *Environ. Sci. Technol.* **2006**, *40* (10), 3148−3155.
(80) Wu, Z.; Hu, M.; Lin, P.; Liu, S.; Wehner, B.; Wiedensohler, A. Particle number size distribution in the urban atmosphere of Beijing, China. *Atmos. Environ.* **2008**, *42* (34), 7967−7980.



DOI: 10.1021/acs.est.6b05724
*Environ. Sci. Technol.* 2017, 51, 3767−3775